A study of vorticity formation in high energy nuclear collisions

(Eur. Phys. J. C75 (2015) 9, 406)

F. Becattini[1 2] G. Inghirami[3 4] V. Rolando [5 6] A. Beraudo [7] L. Del Zanna [1 2 8] A. De Pace [7] M. Nardi [7] G. Pagliara [5 6] V. Chandra [9]

[1]Dipartimento di Fisica e Astronomia, Università di Firenze, Italy [2]INFN - Sezione di Firenze, Italy [3]Frankfurt Institute for Advanced Studies (FIAS), Germany [4]Johann Wolfgang Goethe University, Frankfurt am Main, Germany
[5]Dipartimento di Fisica e Scienze della Terra, Università di Ferrara, Italy [6]INFN - Sezione di Ferrara, Italy [7]INFN - Sezione di Torino, Italy [8]INAF - Oss. Astrofisico di Arcetri, Italy [9]Indian Institute of Technology Gandhinagar, India

Introduction

Vorticity in peripheral collisions[1, 2, 3] provides information about the (mean) hydrodynamic initial conditions and it is related to the onset of peculiar physics in the plasma at high temperature, such as the chiral vortical effect [4]. It has been shown that vorticity gives rise to polarization of particles in the final state, so that e.g. Λ baryon polarization can be used to detect it [5, 6]. In relativistic hydrodynamics, one can define several vorticities:

- Kinematical vorticity: $\omega_{\mu\nu} = \frac{1}{2}(d_\nu u_\mu - d_\mu u_\nu) = \frac{1}{2}(\partial_\nu u_\mu - \partial_\mu u_\nu)$
- T-vorticity: $\Omega_{\mu\nu} = \frac{1}{2}[\partial_\nu(Tu_\mu) - \partial_\mu(Tu_\nu)]$
- Thermal vorticity: $\varpi_{\mu\nu} = \frac{1}{2}(\partial_\nu\beta_\mu - \partial_\mu\beta_\nu)$

each having peculiar features.
Particularly,

- for an ideal uncharged fluid, T-vorticity vanishes if it vanishes in the initial state, unlike kinematical and thermal vorticity.
- thermal vorticity is constant at full thermodynamical equilibrium and in local thermodynamical equilibrium drives particle polarization.

Modeling of the initial conditions

We have studied vorticity formation with our ECHO-QGP 3+1 D code [7] implementing relativistic dissipative hydrodynamics in the Israel-Stewart formulation with minimal Bjorken initial conditions (i.e. with $u^x = u^y = u^\eta = 0$) and with an initial energy density $\varepsilon(x, y, \eta)$ modified with a function $f(\eta)$, being η the longitudinal Bjorken coordinate, such as to have a finite angular momentum [8].

$$f_-(\eta) = \begin{cases} 1 & \eta < -\eta_m \\ \dfrac{-\eta + \eta_m}{2\eta_m} & -\eta_m \le \eta \le \eta_m \\ 0 & \eta > \eta_m \end{cases}$$

$$f_+(\eta) = \begin{cases} 0 & \eta < -\eta_m \\ \dfrac{\eta + \eta_m}{2\eta_m} & -\eta_m \le \eta \le \eta_m \\ 1 & \eta > \eta_m \end{cases}$$

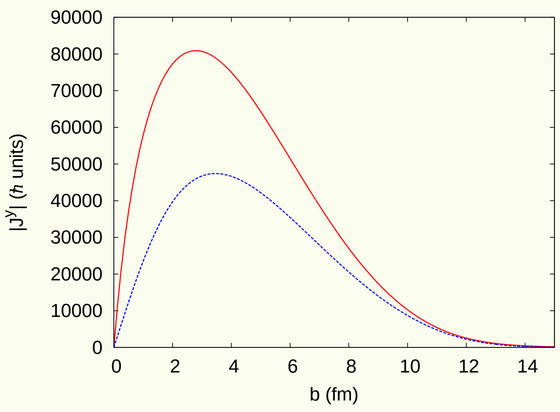

Figure 1 : Estimated angular momentum (in $\hbar$ units) of the overlap region of the two colliding nuclei (solid line) and total angular momentum of the plasma according to the parametrization of the initial conditions (dashed line), as a function of the impact parameter b.

Validation of the code used for this study

To validate the core routines of our ECHO-QGP code, we performed a numerical simulation of a Bjorken conformal flow with an azimuthally symmetric radial expansion and we compared the results with the semi-analytic solutions that extend to the viscous case [13, 14] the solutions previously found by Gubser and Yarom [11, 12] in the unviscid case.

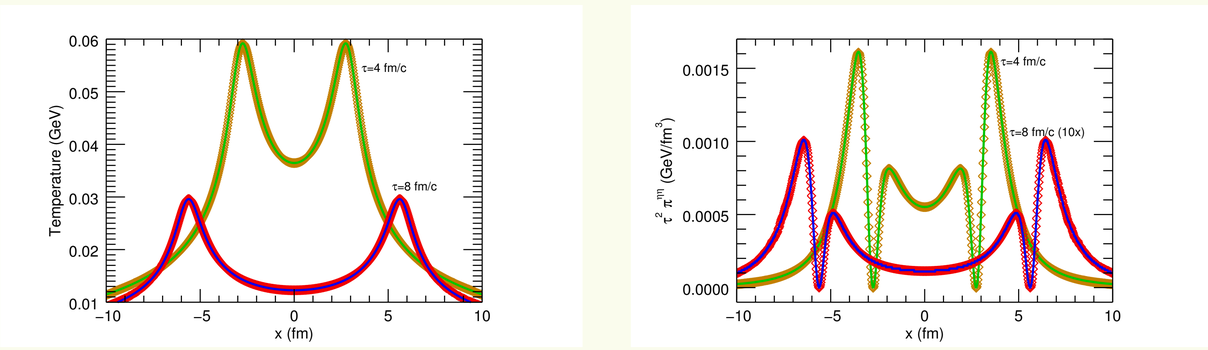

Figure 2 : Comparison between the semi-analytic solution of the Gubser viscous flow (solid lines) and the numerical ECHO-QGP computation (dots). The simulation has been performed with a grid of 0.025 fm in space and 0.001 fm in time.

We validated vorticity computations by checking that T-vorticity vanishes in the unviscid case, as a function of grid spacing and of introduced viscosity.

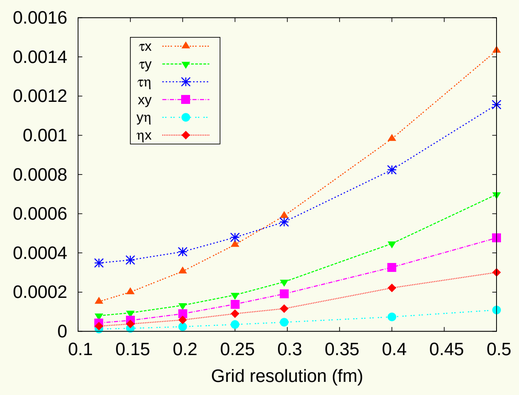

Figure 3 : Mean of the absolute value of T-vorticity components, divided by T^2, at the freeze-out as a function of the grid resolution.

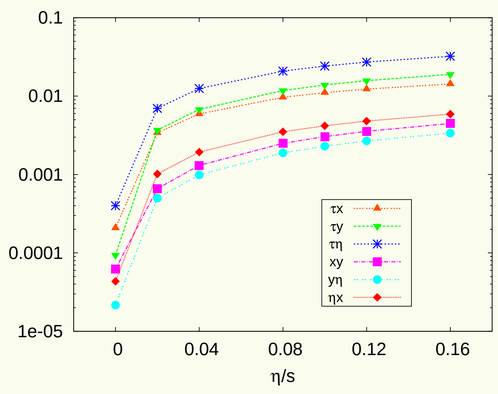

Figure 4 : Mean of the absolute values of $\Omega_{\mu\nu}/T^2$ components at the freeze-out hypersurface as a function of η/s. Note that the $\Omega_{x\eta}, \Omega_{y\eta}, \Omega_{\tau\eta}$ have been multiplied by $1/\tau$. Left: log scale. Right: zoom on the zero region.

Sensitivity to η/s

The free parameters have been chosen following ref. [9], where they were adjusted to reproduce the data in Au-Au collisions at $\sqrt{s_{NN}} = 200$ GeV. The values of η_m and η/s have been chosen to obtain (qualitatively) the best agreement between our calculated pion $v_1(y)$ and the measured directed flow for charged particles in the central rapidity region by the STAR collaboration [10].

Parameter	Value
$\sqrt{s_{NN}}$	200 GeV
α	0.
ϵ_0	30 GeV/fm^3
σ_{in}	40 mb
τ_0	0.6 fm/c
η_{flat}	1
σ_η	1.3
T_{fo}	130 MeV
b	11.57fm
η_m ideal	3.36
η_m viscous	2.0
η/s	0.1

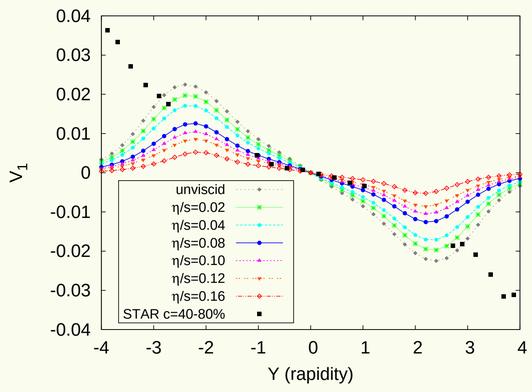

Figure 5 : $v_1(y)$ of $\pi^\pm$ for different values of η/s with $\eta_m = 2.0$, compared with STAR data [10].

Results on thermal vorticity and polarization

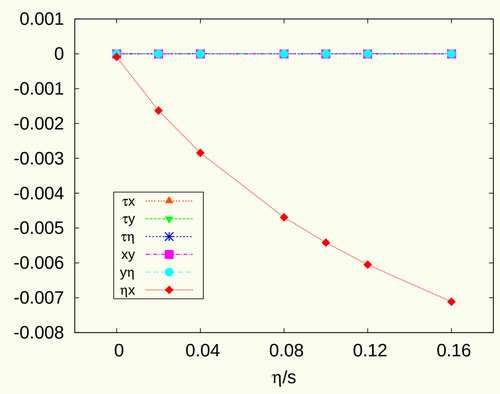

Figure 6 : Mean values of thermal vorticity components at the freeze-out *vs* η/s. $\varpi_{x\eta}\varpi_{y\eta}, \varpi_{\tau\eta}$ are multiplied by $1/\tau$.

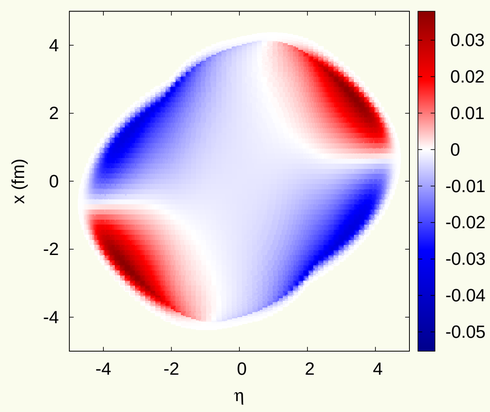

Figure 7 : $1/\tau$-scaled ηx cov. component of the thermal vorticity, $\varpi_{\eta x}/\tau$ over the freeze-out hypersurf. for $y = 0$, η/s=0.1, η_m=2.0.

The relation between the polarization vector of a spin 1/2 particle and thermal vorticity is [5]:

$$\Pi^\mu(p) = \frac{1}{8m}\frac{\int_\Sigma d\Sigma_\lambda p^\lambda n_F(1-n_F)\, p_\sigma \epsilon^{\mu\nu\rho\sigma}\partial_\nu\beta_\rho}{\int_\Sigma d\Sigma_\lambda p^\lambda\, n_F} \tag{1}$$

but the polarization vector which is measurable is the one in the decaying particle rest frame:

$$\Pi_0^0 = \frac{\epsilon}{m}\Pi^0 - \frac{\mathbf{p}\cdot\mathbf{\Pi}}{m} \qquad \mathbf{\Pi}_0 = \mathbf{\Pi} - \frac{\mathbf{p}\cdot\mathbf{\Pi}}{\epsilon(m+\epsilon)}\mathbf{p} \tag{2}$$

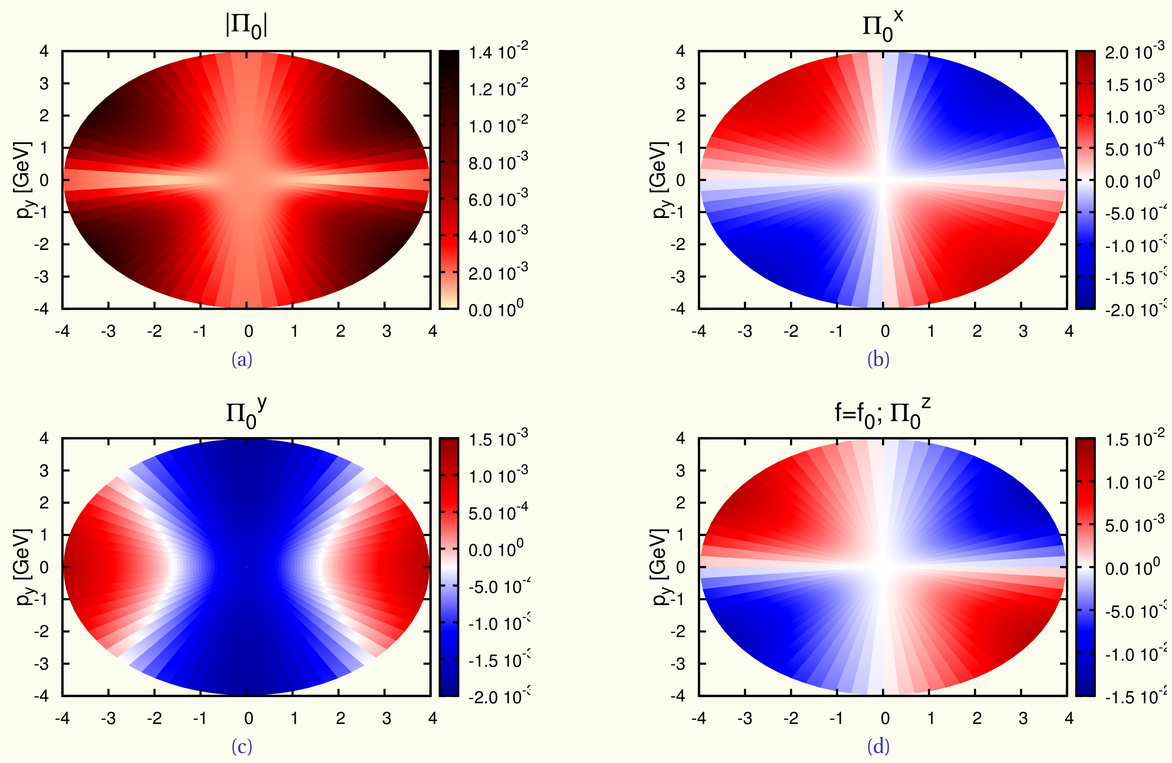

Figure 8 : Magnitude (panel a) and components (panels b,c,d) of the polarization vector of the Λ hyperon in its rest frame.

References

[1] F. Becattini, F. Piccinini and J. Rizzo, Phys. Rev. C **77** (2008) 024906.

[2] L. P. Csernai, V. K. Magas and D. J. Wang, Phys. Rev. C **87** (2013) 034906.

[3] L. P. Csernai, D. J. Wang, M. Bleicher and H. Stöcker, Phys. Rev. C **90** (2014) 021904.

[4] D. E. Kharzeev and D. T. Son, Phys. Rev. Lett. **106** (2011) 062301

[5] F. Becattini, V. Chandra, L. Del Zanna and E. Grossi, Annals Phys. **338** (2013) 32.

[6] F. Becattini, L. Csernai and D. J. Wang, Phys. Rev. C **88** (2013) 3, 034905.

[7] L. Del Zanna, V. Chandra, G. Inghirami, V. Rolando, A. Beraudo, A. De Pace, G. Pagliara, A. Drago and F. Becattini, Eur. Phys. J. C **73** (2013) 2524.

[8] P. Bozek and I. Wyskiel, Phys. Rev. C **81** (2010) 054902

[9] H. Song and U. W. Heinz, Phys. Rev. C **77** (2008) 064901.

[10] B.I. Abelev *et al.* (STAR Collaboration), Phys. Rev. Lett. 101 (2008), 252301.

[11] S.S. Gubser, Phys. Rev. D 82 (2010) 085027.

[12] S.S. Gubser and A. Yarom, Nucl. Phys. B 846 (2011) 469.

[13] H. Marrochio, J. Noronha, G. S. Denicol, M. Luzum, S. Jeon and C. Gale, Phys. Rev. C **91** (2015) 1, 014903.

[14] G. S. Denicol, U. W. Heinz, M. Martinez, J. Noronha and M. Strickland, Phys. Rev. D **90** (2014) 12, 125026.

INFN Istituto Nazionale di Fisica Nucleare · Università degli Studi Firenze · Università degli Studi di Ferrara · FIAS Frankfurt Institute for Advanced Studies

Pre-print article:
http://arxiv.org/abs/1501.04468
ECHO-QGP website:
http://theory.fi.infn.it/echoqgp/